





# Radiomics in advanced gastroenteropancreatic neuroendocrine neoplasms: Identifying responders to somatostatin analogs

Michela Polici<sup>1</sup> | Damiano Caruso<sup>1</sup> | Benedetta Masci<sup>1</sup>  | Matteo Marasco<sup>2</sup>  |  
Daniela Valanzuolo<sup>1</sup> | Elisabetta Dell'Unto<sup>2</sup> | Marta Zerunian<sup>1</sup> |  
Davide Campana<sup>3</sup> | Domenico De Santis<sup>1</sup> | Giuseppe Lamberti<sup>3</sup>  |  
Elsa Iannicelli<sup>1</sup> | Daniela Prosperi<sup>4</sup> | Bruno Annibale<sup>2</sup> | Andrea Laghi<sup>1</sup> |  
Francesco Panzuto<sup>2</sup>  | Maria Rinzivillo<sup>2</sup>

<sup>1</sup>Department of Medical-Surgical Sciences and Translational Medicine, ENETS Center of Excellence, Radiology Unit, Sant'Andrea University Hospital, Sapienza University of Rome, Rome, Italy

<sup>2</sup>Department of Medical-Surgical Sciences and Translational Medicine, ENETS Center of Excellence, Digestive Disease Unit, Sant'Andrea University Hospital, Sapienza University of Rome, Rome, Italy

<sup>3</sup>Department of Medical and Surgical Sciences (DIMEC), Medical Oncology Unit, Alma Mater Studiorum—University of Bologna, IRCCS Azienda Ospedaliero-Universitaria di Bologna, Bologna, Italy

<sup>4</sup>ENETS Center of Excellence, Nuclear Medicine Unit, Sant'Andrea University Hospital, Sapienza University of Rome, Rome, Italy

## Correspondence

Francesco Panzuto, Department of Medical-Surgical Sciences and Translational Medicine, ENETS Center of Excellence, Sapienza University of Rome, Via Giorgio Papanicolau snc, Rome 00189, Italy.  
Email: [francesco.panzuto@uniroma1.it](mailto:francesco.panzuto@uniroma1.it)

## Funding information

Open access publishing facilitated by Università degli Studi di Roma La Sapienza, as part of the Wiley–CRUI–CARE agreement

## Abstract

To evaluate a radiomic strategy for predicting progression in advanced gastroenteropancreatic neuroendocrine tumor (GEP-NET) patients treated with somatostatin analogs (SSAs). Fifty-eight patients with GEP-NETs and liver metastases, with baseline computerized tomography (CT) scans from June 2013 to November 2020, were studied retrospectively. Data collected included progression-free survival (PFS), overall survival (OS), tumor grading, death, and Ki67 index. Patients were categorized into progressive and non-progressive groups. Two radiologists performed 3D liver segmentation on baseline CT scans using 3DSlicer v4.10.2. One hundred six radiomic features were extracted and analyzed (*T*-test or Mann–Whitney). Radiomic feature efficacy was evaluated via receiver operating characteristic curves, and both univariate and multivariate logistic regression were used to develop predictive models. A significance level of  $p < .05$  was maintained. Of 55 patients, 38 were progressive (median PFS and OS: 14 and 34 months, respectively), and 17 were non-progressive (median PFS and OS: 58 months each). Six radiomic features significantly differed between groups ( $p < .05$ ), with an area under the curve (AUC) range of 0.64–0.74. Ki67 was the only clinical parameter significantly associated with progression risk (odds ratio (OR) = 1.14,  $p < .05$ ). The combined radiomic features and Ki67 model proved most effective, showing an AUC of 0.814 ( $p = .008$ ). The radiomic model alone did not reach statistical significance ( $p = .07$ ). A combined model incorporating radiomic features and the Ki67 index effectively predicts disease progression in GEP-NET patients eligible for SSA treatment.

## KEYWORDS

lanreotide, neuroendocrine tumors, octreotide, prognosis, radiomic

Michela Polici and Damiano Caruso contributed equally to the study.

This is an open access article under the terms of the [Creative Commons Attribution-NonCommercial](https://creativecommons.org/licenses/by-nc/4.0/) License, which permits use, distribution and reproduction in any medium, provided the original work is properly cited and is not used for commercial purposes.

© 2024 The Author(s). *Journal of Neuroendocrinology* published by John Wiley & Sons Ltd on behalf of British Society for Neuroendocrinology.

## 1 | INTRODUCTION

Neuroendocrine neoplasms (NENs) are rare and heterogeneous diseases whose prognosis depends on several factors, including the primary tumor site, tumor grading, disease staging, and the expression of somatostatin receptors.<sup>1,2</sup> Among these, tumor grade is widely considered the strongest prognostic factor, capable of predicting patient survival and response probability to medical treatments. It is usually assessed by evaluating the Ki67 immunohistochemical proliferative activity. This method discriminates well-differentiated neuroendocrine tumors (NET) into G1 grade (Ki67 lower than 3%), G2 grade (Ki67 3%–20%), and G3 grade (Ki67 higher than 20%). When the tumor exhibits poorly differentiated morphology, it is termed neuroendocrine carcinoma (NEC), which, by definition, has high proliferative activity (G3 grade).<sup>3</sup> Although Ki67 is adept at predicting clinical outcomes, it has limitations due to potential heterogeneity within the same lesion, differences between primary tumors and metastatic sites, and assessment challenges related to low tissue availability, especially in advanced disease where tissue sampling often relies on a single biopsy obtained via percutaneous or endoscopic-ultrasonography approach.<sup>4</sup>

The therapeutic landscape for advanced NEN includes somatostatin analogs (SSAs), targeted agents, radioligand therapy (RLT), and systemic chemotherapy. Selecting the optimal therapeutic sequence can be challenging due to the disease above heterogeneity. However, it is well-recognized that SSAs are the first-line treatment in advanced, well-differentiated G1-G2 gastroenteropancreatic (GEP) NETs expressing somatostatin receptors.<sup>5</sup> In this context, SSAs have been shown to inhibit tumor growth in 50%–80% of patients, as demonstrated by phase-3 randomized controlled trials.<sup>6,7</sup> Since this scenario represents approximately 70% of cases, SSAs are commonly considered the initial therapeutic approach for most GEP-NET patients. Nonetheless, despite favorable prognostic factors, a proportion of well-differentiated GEP-NETs exhibit a disappointing response to SSAs, showing progression after a few months of therapy. Early identification of these patients is crucial for physicians managing these cases, as it allows for planning stricter follow-ups and an early switch to more effective second-line treatments, including RLT.

Through radiomic analysis, quantitative imaging is emerging as a potential new imaging biomarker in oncology, particularly for identifying NEN patients with poorer prognoses and unfavorable outcomes. This approach analyzes medical images to extract numerous numerical parameters that reflect the microarchitecture and heterogeneity of tumors.<sup>8</sup> While not replacing traditional tumor profiling methods, radiomics is a supplementary tool, bridging the gap between generic and personalized medicine. Recent studies highlight its effectiveness in tumor grading, differential diagnosis, and predicting responses to Everolimus in GEP-NETs.<sup>8–11</sup> These findings suggest that radiomics could enhance cancer profiling and minimize the risks of subjective bias in clinical assessments.<sup>8–10</sup> However, data on the ability of radiomics to predict the efficacy of SSAs are currently lacking in the literature.

In this study, we aimed to investigate the potential value of radiomics in identifying patients with advanced GEP-NETs who are at a higher risk of non-response to SSA therapy.

## 2 | MATERIALS AND METHODS

### 2.1 | Study design

This retrospective observational study was in line with the Declaration of Helsinki. All steps of recruitment and data collecting were approved by the ENETS Center of Excellence—Sant'Andrea University Hospital, Rome. The data for this study were analyzed as part of the data entered in the NET database, approved by the ethical committee of the ENETS Center of Excellence S. Andrea (CE 5454\_2019); informed consensus for data collection was obtained from all patients. The population was created among patients with advanced GEP-NETs, with a particular focus on liver metastases, screened from the ENETS Center of Excellence repository of Rome and Bologna from July 2013 to November 2020. Clinical-epidemiological data (sex, age, tumor grading, primary, and Ki67) and outcome data (date of progression, progression-free survival [PFS], and overall survival [OS]) were collected.

All patients were selected following the inclusion criteria: (I) histological diagnosis of well-differentiated G1-G2 GEP-NETs, (II) presence of liver metastases, (III) availability of contrast-enhanced baseline CT scans, and (IV) clinical history of SSAs used as first-line therapy. The exclusion criteria were (I) previous liver locoregional treatment, (II) patients with grading G3 according to WHO classification, and (III) SSAs associated with other therapies.

The occurrence of progression was evaluated according to RECIST 1.1 criteria<sup>12</sup> in the follow-up CT scans by an expert oncological expert radiologist with RECIST Qualification (DC). PFS was assessed from the time the SSAs' treatment began. Although the methods and timing of follow-up were not pre-determined as this was a retrospective study, the follow-up was conducted according to the ENETS recommendations<sup>13,14</sup> and the protocols adopted by the Center of Excellence. These included an initial radiological check with computerized tomography (CT) or magnetic resonance imaging (MRI) after 3–6 months from the start of treatment, followed by the repetition of the same exams with chest and abdominal studies every 6–12 months, depending on the specific characteristics of the tumor. Starting from an initial population of 84 patients, the final population of 55 patients with liver metastases in GEP-NETs was selected and treated with SSAs upfront, with grading G1 and G2.

### 2.2 | CT acquisition protocol

All patients underwent baseline contrast-enhanced CT scans. The exams were performed by using 128-slices CT (GE Revolution EVO Slice CT Scanner, GE Healthcare, Milwaukee, WI, USA) with the participants in the supine position. The scans were made in inspiration, in cranio-caudal direction, including the entire abdomen for all phases: unenhanced, late arterial, and portal venous.

The amount of contrast medium (CM) was calculated by lean body weight (LBW),<sup>15,16</sup> according to the following formula:

$$\text{CM volume (mL)} = \frac{0.7 \text{gl} \times \text{LBW (kg)}}{\text{CM concentration} \left( \frac{\text{mgI}}{\text{mL}} \right)}$$

The contrast media injection system (MEDRAD® Centargo CT Injection System) was used for CM administration in bolus (Iomeprol 400 mg I/mL, Iomeron 400; Bracco Imaging) and the saline solution (40 mL) through an antecubital venous access (18–20 gauge) with a flow rate of 3/3.5 mL/s. For all CT scans, the bolus-tracking method (Smart Prep, GE, Milwaukee, WI) was used, which outlines the region of interest at the level of the celiac tripod in the abdominal aorta, setting 150 HU-threshold. All CT scans were performed with a multi-phase protocol: unenhanced phase, a delay of 18 for the late arterial phase, and a delay of 70 s for the portal venous phase. For all exams were set specific technical parameters: 100 kV tube voltage; 130–300 mAs for the automatic current modulation by using Auto-mAs (GE Healthcare, Milwaukee, USA); 0.625 × 64 mm for the collimation; 0.984:1 of spiral pitch factor, 0.6 s of gantry speed. Iterative Reconstruction at 40% (ASiR-V, GE Healthcare, Milwaukee, USA) was used for all standard soft tissue reconstruction at 1.25 of slice thickness.

### 2.3 | CT scan segmentation analysis

The volumetric liver segmentations were performed by two abdominal expert radiologists independently for all baseline CT scans through a dedicated open-source software (3D Slicer software, version 4.10.2, <http://www.slicer.org>). All segmentations were performed manually, slice by slice, on the late arterial phase based on literature data,<sup>9,10</sup> avoiding any principal liver vessels and the main bile duct (Figure 1).

### 2.4 | Radiomic features extraction

One hundred and seven radiomic features were extracted from all segmentations using a dedicated extension of 3D Slicer Radiomics (radiomics library),<sup>17</sup> among these were both shape and first- and second-order parameters: 2D and 3D Shape 13 features, First-Order statistics 19 features, Gray Level Dependence Matrix (GLDM)

14 features, Gray Level Size Zone Matrix (GLSZM) 16 features, Gray Level Co-Occurrence Matrix (GLCM) 24 features, Neighboring Gray Tone Difference Matrix (NGTDM) 5 features, Gray Level Run Length Matrix (GLRLM) 16 features. Among GLDM features, the Gray Level Non-Uniformity Normalized was excluded according to the investigations on redundancy and similarity performed and published by pyradiomics (<https://pyradiomics.readthedocs.io>).

### 2.5 | Statistical analysis

Statistical analyses were performed with MedCalc (MedCalc Software, version 15, Ostend, Belgium). The radiomic features were reduced with interobserver variability to identify only the stable features, considering unstable the values of intraclass correlation coefficient (ICC) < 0.75, stable 0.75 ≤ ICC < 0.9, and very good ICC ≥ 0.9. All continuous variables were expressed as mean ± standard deviation, and the comparisons were performed with the Student's *T*-test and Mann-Whitney *U* test, according to Gaussian normality or not, respectively. All categorical variables were expressed with numbers and percentages. The radiomic features were significantly compared to the two groups tested with the receiver operating curve (ROC) to express the area under the curve (AUC), sensitivity, specificity, and cut-off values having the progression as an endpoint.

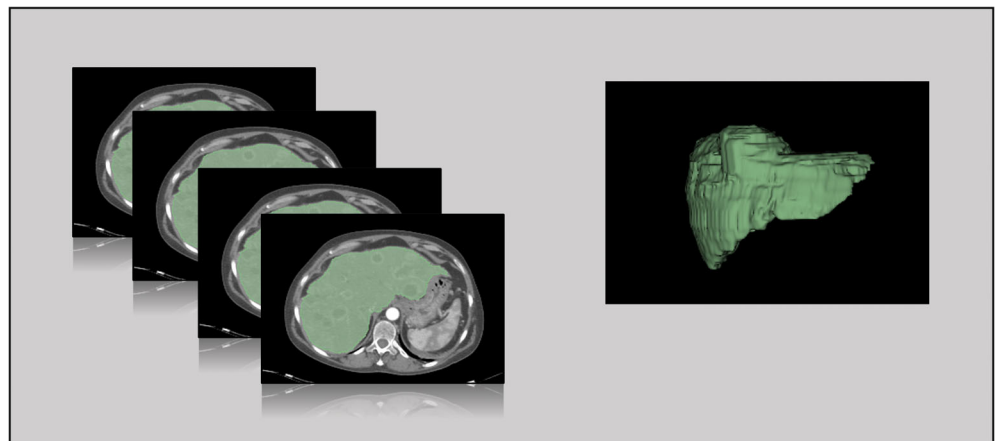
The univariate enter logistic regression analysis was applied for all clinical and radiomic features to predict the progression from the baseline CT scans. The features with significant results (*p* < .05) were entered in the multivariable enter logistic regression analysis to build the predictive models: radiomic and combined models. The value of *p* < .05 was the reference to assess the statistical significance.

## 3 | RESULTS

### 3.1 | Study population

The final population includes 55 patients (median age: 54 years), including 25/55 pancreatic NETs (45.5%) and 30/55 ileal NETs

**FIGURE 1** The 3D manual segmentation of metastatic liver performed on the arterial phase of baseline CT scans.



(54.5%). Concerning the grading, 35/55 were G2 NETs (63.6%), and 20/5 were G1 NETs (36.4%) (Table 1). All patients had liver metastases 55/55 (100%), and 14/55 (25.5%) patients also had concomitant extra-liver metastases (lymph nodes, 8 patients; bone 4 patients; peritoneum, 4 patients). All patients had positive results at Ga<sup>68</sup>-DOTA-TOC-PET/CT before starting SSAs. Concerning the treatment, 26/55 (47.3%) were treated with lanreotide and 29/55 (52.7%) with octreotide. No patient received an above-standard dose of SSA.

According to follow-up data, the population was divided into two groups: 38/55 progressive (69%) and 17/55 non-progressive (31%) (Figure 2). Among the 55 patients studied, the progressive group (38/55) comprised 17 (30.9%) with ileal primary tumors and 21 (38.1%) with pancreatic primary tumors. In contrast, the non-progressive group (17/55) included 13 (23.6%) patients with ileal NETs and only

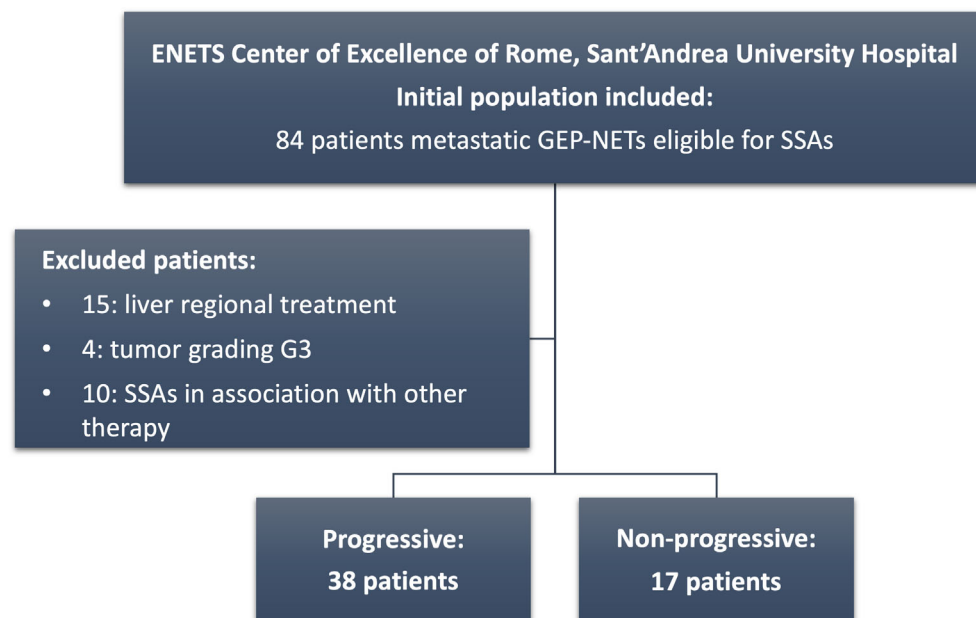
4 (7.27%) with pancreatic primary tumors. Of the 55 patients included, baseline chromogranin A (CgA) levels were available in 37 patients (67% of the cohort), with a median value of 197 ng/mL (CI 76–238; normal range 19–98 ng/mL). The median Ki67 in the progressive group was 8%; in this group, the median PFS was 14 months, and the median OS was 34 months. In the non-progressive group, the median Ki67 was 2.5%; the median PFS and OS were 58 months each. In the general population, it was observed that 26 of 55 patients died during the follow-up, resulting in a mortality rate of 47.3%.

### 3.2 | Radiomic features selection and performance

Among the 106 radiomic features extracted from the liver 3D segmentations performed during the late arterial phase, 12 of 106 features showed an ICC in the range of 0.75 to <0.9, indicating stability or an ICC of 0.9 or higher, indicating very good reliability. These were compared between responders and non-responders; of the 12 radiomic features analyzed, 7 showed significant differences with  $p < .05$  (Table 2). Concerning the ROC curves, six features had significant results: the Surface Volume Ratio (Shape), with AUC of 0.711 ( $p = .006$ ), specificity = 66.7% and sensitivity = 75%; Large Dependence High Gray Level Emphasis (GLDM), with AUC of 0.69 ( $p = .01$ ), specificity = 88.9% and sensitivity = 50%; Low Gray Level Emphasis (GLDM), with AUC of 0.66 ( $p = .02$ ), specificity = 44.5% and sensitivity = 84.4%; Long Run High Gray Level Emphasis (GLRLM), with AUC of 0.69 ( $p = .01$ ), specificity = 78.8% and sensitivity = 56.3%; Short Run Low Gray Level Emphasis (GLRLM), with AUC of 0.64 ( $p = .02$ ), specificity = 33.4% and sensitivity = 93.8%; Large Area High Gray Level Emphasis (GLSZM), with AUC of 0.736 ( $p = .003$ ), specificity = 55.6% and sensitivity = 90.61% (Figure 3, Table 3).

**TABLE 1** Patient general features.

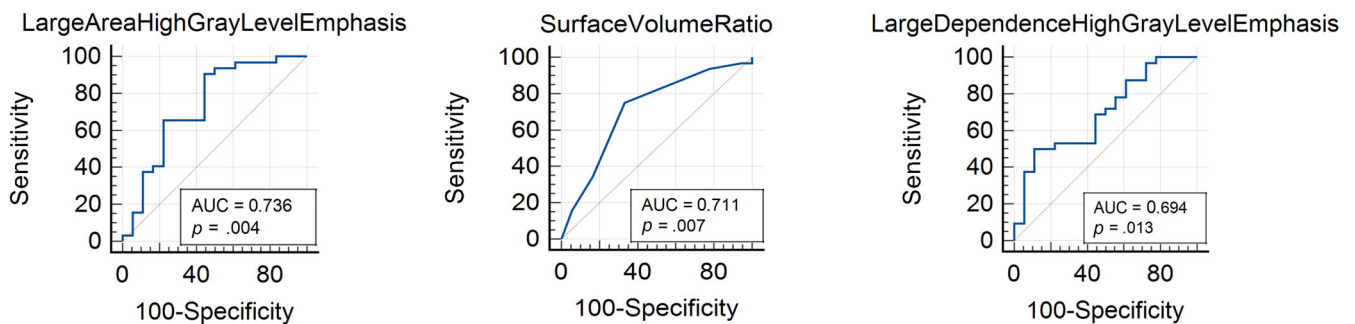
Patients characteristics	Patients (n = 55)	%
Male	28	50.9
Primary tumor site		
Pancreas	25	45.5
Ileum	30	54.5
Grading		
NET G1	20	36.4
NET G2	35	63.6
Functional status		
Functioning	16	29
Non-functioning	39	71
Progressive disease	38	69
Non-progressive disease	17	31



**FIGURE 2** Flowchart of patient enrollment and study design.

**TABLE 2** Significant radiomic features resulted in a comparison between progressive and non-progressive GEP-NETs.

Radiomic features	Progressive Mean ± SD	Non-progressive Mean ± SD	<i>p</i>	ICC
Shape_SurfaceVolumeRatio	0.06 ± 0.02	0.07 ± 0.01	0.01	0.87
GLDM_LargeDependenceHighGrayLevelEmphasis	90,178 ± 30,472	64,838 ± 33,535	0.009	0.92
GLDM_LowGrayLevelEmphasis	0.005 ± 0.002	0.02 ± 0.048	0.01	0.82
GLRLM_LongRunHighGrayLevelEmphasis	5580.8 ± 5336.6	3008.1 ± 2407.4	0.02	0.85
GLRLM_ShortRunLowGrayLevelEmphasis	0.003 ± 0.001	0.011 ± 0.022	0.01	0.93
GLSZM_LargeAreaHighGrayLevelEmphasis	881,085,385 ± 882,877,721	504,018,669 ± 468,447,533	0.006	0.86
GLSZM_ZoneEntropy	5.14 ± 0.39	4.75 ± 0.76	0.01	0.91

**FIGURE 3** The best ROC curves of significant radiomic features in the comparison between progressive and non-progressive advanced GEP-NETs treated with SSAs alone.**TABLE 3** Performance of radiomic parameters in comparison between progressive and non-progressive NETs tested by using receiver operating characteristic (ROC) curve.

Radiomic features	Progressive versus non-progressive			Criterion	<i>p</i>
	Sensitivity (%)	Specificity (%)	AUC		
Shape_SurfaceVolumeRatio	75	66.7	0.72	≤0.06	0.006
GLDM_LargeDependenceHighGrayLevelEmphasis	50	88.9	0.69	>87,981	0.01
GLDM_LowGrayLevelEmphasis	84.4	44.5	0.66	≤0	0.02
GLRLM_LongRunHighGrayLevelEmphasis	56.3	77.8	0.69	>3388.7	0.01
GLRLM_ShortRunLowGrayLevelEmphasis	93.7	33.4	0.64	≤0	0.02
GLSZM_LargeAreaHighGrayLevelEmphasis	90.6	55.6	0.74	>359,709,392	0.003
GLSZM_ZoneEntropy	-	-	-	-	0.06

### 3.3 | Univariate and multivariate analyses

Univariate logistic regression was used to assess the correlation with progression among all stable radiomic features, Ki67, and sex. Six radiomic features—Elongation, Minor Axis Length, Maximum, Mean, Range, and Complexity—demonstrated independent correlations with progressive disease, with *p*-values ranging from 0.02 to 0.04. Specifically, one Shape feature (Elongation) and two First-Order features (Mean and Minor Axis Length) showed a direct correlation with progressive disease, with odds ratios (ORs) ranging from 1.03 to 38.14 ( $p < .05$ ). Conversely, two First-Order features (Range, Maximum) and one NGTDM feature (Complexity) exhibited an inverse correlation

with progressive disease, with ORs ranging from 0.78 to 0.97 ( $p < .05$ ). Among the clinical parameters, only Ki67 demonstrated an independent correlation with progression, with an OR of 1.14 (95% CI 1.05–1.28) and  $p = .01$ . Non-significant results were found for sex ( $p = .47$ ) and age ( $p = .08$ ).

Multivariate logistic regression was conducted to develop radiomic and combined models, using progression as the endpoint. The combined model, incorporating both Ki67 and radiomics, yielded significant results with a *p*-value of 0.008, an AUC of 0.814, and an estimated classification accuracy of 74.55%. In contrast, the radiomic model alone produced non-significant results with a *p*-value of 0.07 (Table 4).

Variable	Univariate analysis		Combined model	
	OR (95%CI)	<i>p</i>	OR (95%CI)	<i>p</i>
Age	-	0.08	-	-
Sex ( <i>F</i> = 0)	-	0.47	-	-
Ki67	1.14 (1.01-1.28)	0.01	1.2 (1.01-1.4)	0.02
Shape_Elongation	38.14 (0.038-37,813.9)	0.03	-	-
Shape_MinorAxisLength	1.23 (1.01-1.35)	0.04	-	-
First-Order_Maximum	0.97 (0.96-1)	0.04	0.98 (0.97-0.99)	0.01
First-Order_Mean	1.03 (0.98-1.06)	0.034	-	-
First-Order_Range	0.78 (0.73-1.3)	0.006	1.11 (1.03-1.2)	0.01
NGTDM_Complexity	0.97 (0.96-1.1)	0.02	-	-
			AUC	0.814
			<i>p</i>	0.008

Abbreviations: NGTDM, Neighboring Gray Tone Difference Matrix; OR, odds ratio.

## 4 | DISCUSSION

This study demonstrated that an integrated model combining radiomics with clinical-histological parameters could identify patients at risk of progression to SSAs among new diagnoses of advanced GEP-NETs. The population was stratified into progressive and non-progressive groups based on progression during follow-up, and all baseline CT scans were analyzed to extract radiomic features from liver segmentations. Our analysis revealed that radiomic parameters and Ki67 could distinguish between progressive and non-progressive diseases. The combination of radiomics and Ki67 demonstrated robust predictive power, with an AUC of approximately 0.814. However, radiomics alone failed to yield significant results in predicting progressive disease, underscoring that quantitative imaging should be regarded as a supportive tool rather than a replacement for conventional approaches.

Radiomics is a powerful tool in oncology, showing promising results across various cancers, particularly in differential diagnosis, prognosis prediction, and treatment response.<sup>8-10</sup> Studies consistently highlight radiomics' ability to enhance the work-up of NETs, from diagnosis to prognosis prediction, surpassing traditional qualitative approaches that may suffer from subjective bias in imaging assessments and limitations of clinical features like Ki67 or grading. Specifically, recent studies have demonstrated significant advancements in predicting tumor grades in pancreatic NETs through radiomic analysis of baseline MR and CT scans, often combined with conventional radiological evaluations.<sup>18-20</sup> Radiomics has also shown encouraging results in differential diagnosis, especially for advanced NETs lacking typical enhancement patterns. It has proven effective in distinguishing pancreatic adenocarcinoma from pancreatic NETs<sup>21</sup> and differentiating between lung cancer and organized pneumonia from lung NETs.<sup>22</sup> A recent study showed that a CT-based radiomic model, when combined with select clinic-radiological features, could effectively predict the aggressiveness of pancreatic NETs. This prediction includes tumor grading, microvascular invasion, and M and N staging based on pre-operative CT scans.<sup>23</sup> The model achieved its best

**TABLE 4** Univariate and multivariate logistic regression to test the correlation of radiomics and clinical data with the progression.

results in predicting metastatic disease and tumor grading, with AUCs ranging from 0.81 to 0.85. However, it yielded slightly weaker results in predicting nodal metastases and microvascular invasion, with AUCs of 0.72 and 0.82, respectively. The negative predictive value remained consistent across all endpoints. This study suggests that integrating radiomics into the oncological workflow, alongside clinical and radiological findings, could mitigate several limitations associated with tumor biopsy and subjective image evaluation, thereby reducing the intrinsic biases of conventional approaches.

Current guidelines recommend SSAs for G1 and G2 GEP-NETs that express somatostatin receptors, particularly for slow-growing tumors.<sup>24,25</sup> If these treatments are ineffective, other options, such as RLT, are preferred over targeted agents and chemotherapy due to their higher likelihood of extending PFS.<sup>26</sup> Recent findings from the NETTER-2 trial have shown that upfront first-line RLT significantly outperforms high-dose analogs in G2 and G3 GEP-NETs.<sup>27</sup> However, the challenge remains in accurately identifying patients most likely to benefit from these therapies, which depends largely on tumor grading, symptomatology, and disease extent. Recent literature highlights promising results from a radiomic approach in identifying Everolimus responders among advanced GEP-NET patients based on naïve CT scans.<sup>9</sup> It was found that radiomics surpassed clinical data in predicting responses to targeted therapy, underscoring the insufficiency of clinical methods alone to characterize tumor microenvironment and aggressiveness fully. This aligns with our study, where a combined radiomics and clinical model demonstrated superior predictive accuracy (measured in AUC) compared to the clinical model alone. We developed all models using baseline CT scans, aiming to use a pre-treatment assessment that integrates ki67—recognized as a critical clinical parameter—with radiomic features extracted from liver segmentations. This approach aims to predict the risk of progressive disease in patients initially eligible for SSA treatment.

The NETs workflow could transition from a traditional approach, often influenced by biases from subjective evaluations and intratumoral Ki67 heterogeneity, to a structured, objective, and innovative

approach that includes radiomics. This method aims to provide quantitative data to clinicians. However, it is essential to understand that radiomics should not replace conventional evaluations but should serve as an additional tool for oncologists. This approach is intended to enable personalized therapy for each patient rather than a one-size-fits-all treatment for the pathology. We are aware that this study has limitations, which include its retrospective nature, small sample size, and the heterogeneity of the population in terms of different primary NETs and tumor gradings. Due to these characteristics of the included population, a comparative subanalysis between ileal and pancreatic primary tumors was not feasible for the predictive analysis of radiomics models. This would have been interesting considering the biological differences between these two disease types based on the primary tumor site.<sup>28</sup> Additionally, the absence of a validation cohort further restricts the robustness of our findings. Future studies should aim to expand the initial population, possibly distinguishing between pancreatic and ileal NETs, and incorporate an external cohort for model validation. Since NETs are rare tumors, assembling a large population is challenging, but a multicentric approach could provide a solution. Moreover, several inherent weaknesses of radiomics must be addressed, such as the lack of standardization and reproducibility. Recent research has shown that CT iterative reconstruction can impact the reproducibility of some textural features.<sup>29</sup> The absence of a multicentric dataset for validating predictive models, the unavailability of a large prospective study, technical difficulties in applying radiomics in clinical settings, and assessing its actual impact on decision-making are significant challenges. In the future, developing algorithms to avoid overlapping and exclude unstable features could mitigate these issues.

In conclusion, our study suggests that a predictive model combining radiomic data with grading may help identify patients with advanced GEP-NETs who are more likely to benefit from SSAs treatment. Radiomics shows potential to play a role in the NETs workflow, possibly contributing to the development of personalized therapeutic approaches and improved patient outcomes. This approach might also assist in the earlier identification of patients less responsive to SSA therapy, potentially allowing for closer follow-up and consideration of alternative first-line treatments. However, further research is needed to validate these findings and determine their clinical applicability.

#### AUTHOR CONTRIBUTIONS

**Michela Polici:** Investigation; writing – original draft; methodology; data curation. **Damiano Caruso:** Conceptualization; data curation; supervision; formal analysis. **Benedetta Masci:** Investigation. **Matteo Marasco:** Investigation. **Daniela Valanzuolo:** Investigation. **Elisabetta Dell'Unto:** Investigation. **Marta Zerunian:** Investigation; formal analysis; methodology. **Davide Campana:** Investigation; data curation. **Domenico De Santis:** Investigation; methodology. **Giuseppe Lamberti:** Investigation. **Elsa Iannicelli:** Investigation; data curation. **Daniela Prosperi:** Investigation; data curation. **Bruno Annibale:** Supervision; resources. **Andrea Laghi:** Supervision; resources. **Francesco Panzuto:** Conceptualization; writing – review and editing; project administration; supervision. **Maria Rinzivillo:** Conceptualization; supervision; project administration.

#### CONFLICT OF INTEREST STATEMENT

The authors declare no conflict of interest.

#### PEER REVIEW

The peer review history for this article is available at <https://www.webofscience.com/api/gateway/wos/peer-review/10.1111/jne.13472>.

#### DATA AVAILABILITY STATEMENT

The data that support the findings of this study are available on request from the corresponding author. The data are not publicly available due to privacy or ethical restrictions.

#### ETHICS STATEMENT

The study was conducted after obtaining consent from the patients for data collection for research purposes and was approved by the ethics committee.

#### ORCID

**Benedetta Masci**  <https://orcid.org/0000-0003-0935-6364>

**Matteo Marasco**  <https://orcid.org/0009-0002-0496-3229>

**Giuseppe Lamberti**  <https://orcid.org/0000-0003-3069-7630>

**Francesco Panzuto**  <https://orcid.org/0000-0003-2789-4289>

#### REFERENCES

1. Dasari A, Shen C, Halperin D, et al. Trends in the incidence, prevalence, and survival outcomes in patients with neuroendocrine tumors in the United States. *JAMA Oncol*. 2017;3(10):1335-1342. doi:10.1001/jamaoncol.2017.0589
2. Panzuto F, Merola E, Pavel ME, et al. Stage IV gastro-entero-pancreatic neuroendocrine neoplasms: a risk score to predict clinical outcome. *Oncologist*. 2017;22(4):409-415. doi:10.1634/theoncologist.2016-0351
3. Rindi G, Mete O, Uccella S, et al. Overview of the 2022 WHO classification of neuroendocrine neoplasms. *Endocr Pathol*. 2022;33(1):115-154. doi:10.1007/s12022-022-09708-2
4. La Rosa S. Diagnostic, prognostic, and predictive role of Ki67 proliferative index in neuroendocrine and endocrine neoplasms: past, present, and future. *Endocr Pathol*. 2023;34(1):79-97. doi:10.1007/s12022-023-09755-3
5. La Salvia A, Modica R, Rossi R, et al. Targeting neuroendocrine tumors with octreotide and lanreotide: key points for clinical practice from NET specialists. *Cancer Treat Rev*. 2023;117:102560. doi:10.1016/j.ctrv.2023.102560
6. Rinke A, Müller HH, Schade-Brittinger C, et al. Placebo-controlled, double-blind, prospective, randomized study on the effect of octreotide LAR in the control of tumor growth in patients with metastatic neuroendocrine midgut tumors: a report from the PROMID Study Group. *J Clin Oncol*. 2009;27(28):4656-4663. doi:10.1200/jco.2009.22.8510
7. Caplin ME, Pavel M, Ćwikła JB, et al. Lanreotide in metastatic enteropancreatic neuroendocrine tumors. *N Engl J Med*. 2014;371(3):224-233. doi:10.1056/nejmoa1316158
8. Caruso D, Polici M, Zerunian M, et al. Radiomics in oncology, part 1: technical principles and gastrointestinal application in CT and MRI. *Cancer*. 2021;13(11):2522. doi:10.3390/cancers13112522
9. Caruso D, Polici M, Rinzivillo M, et al. CT-based radiomics for prediction of therapeutic response to everolimus in metastatic neuroendocrine tumors. *Radiol Med*. 2022;127(7):691-701. doi:10.1007/s11547-022-01506-4
10. Martini I, Polici M, Zerunian M, et al. CT texture analysis of liver metastases in PNETs versus NPNETs: correlation with

- histopathological findings. *Eur J Radiol.* 2020;124:108812. doi:10.1016/j.ejrad.2020.108812
11. Chiti G, Grazzini G, Flammia F, et al. Gastroenteropancreatic neuroendocrine neoplasms (GEP-NENs): a radiomic model to predict tumor grade. *Radiol Med.* 2022;127(9):928-938. doi:10.1007/s11547-022-01529-x
  12. Eisenhauer E, Therasse P, Bogaerts J, et al. New response evaluation criteria in solid tumours: revised RECIST guideline (version 1.1). *Eur J Cancer.* 2009;45(2):228-247. doi:10.1016/j.ejca.2008.10.026
  13. Sundin A, Arnold R, Baudin E, et al. ENETS consensus guidelines for the standards of care in neuroendocrine tumors: radiological, nuclear medicine and hybrid imaging. *Neuroendocrinology.* 2017;105(3):212-244. doi:10.1159/000471879
  14. Dromain C, Vullierme M, Hicks RJ, et al. ENETS standardized (synoptic) reporting for radiological imaging in neuroendocrine tumours. *J Neuroendocrinol.* 2021;34(3):e13044. doi:10.1111/jne.13044
  15. Caruso D, Rosati E, Panvini N, et al. Optimization of contrast medium volume for abdominal CT in oncologic patients: prospective comparison between fixed and lean body weight-adapted dosing protocols. *Insights Imaging.* 2021;12(1):40. doi:10.1186/s13244-021-00980-0
  16. Caruso D, De Santis D, Rivosecchi F, et al. Lean body weight-tailored iodinated contrast injection in obese patient: Boer versus James formula. *Biomed Res Int.* 2018;2018:8521893. doi:10.1155/2018/8521893
  17. Van Griethuysen JJ, Fedorov A, Parmar C, et al. Computational radiomics system to decode the radiographic phenotype. *Cancer Res.* 2017;77(21):e104-e107. doi:10.1158/0008-5472.can-17-0339
  18. Zhu HB, Zhu HT, Jiang L, et al. Radiomics analysis from magnetic resonance imaging in predicting the grade of nonfunctioning pancreatic neuroendocrine tumors: a multicenter study. *Eur Radiol.* 2023;34(1):90-102. doi:10.1007/s00330-023-09957-7
  19. Ye JY, Fang P, Peng ZP, Huang XT, Xie JZ, Yin XY. A radiomics-based interpretable model to predict the pathological grade of pancreatic neuroendocrine tumors. *Eur Radiol.* 2023;34:1994-2005. doi:10.1007/s00330-023-10186-1
  20. Javed AA, Zhu Z, Kinny-Köster B, et al. Accurate non-invasive grading of nonfunctional pancreatic neuroendocrine tumors with a CT derived radiomics signature. *Diagn Interv Imaging.* 2024;105(1):33-39. doi:10.1016/j.diii.2023.08.002
  21. He M, Liu Z, Lin Y, et al. Differentiation of atypical non-functional pancreatic neuroendocrine tumor and pancreatic ductal adenocarcinoma using CT based radiomics. *Eur J Radiol.* 2019;117:102-111. doi:10.1016/j.ejrad.2019.05.024
  22. Adelsmayr G, Janisch M, Müller H, et al. Three dimensional computed tomography texture analysis of pulmonary lesions: does radiomics allow differentiation between carcinoma, neuroendocrine tumor and organizing pneumonia? *Eur J Radiol.* 2023;165:110931. doi:10.1016/j.ejrad.2023.110931
  23. Mori M, Palumbo D, Muffatti F, et al. Prediction of the characteristics of aggressiveness of pancreatic neuroendocrine neoplasms (Pan-NENs) based on CT radiomic features. *Eur Radiol.* 2022;33(6):4412-4421. doi:10.1007/s00330-022-09351-9
  24. Kos-Kudła B, Castaño JP, Denecke T, et al. European neuroendocrine tumour society (ENETS) 2023 guidance paper for nonfunctioning pancreatic neuroendocrine tumours. *J Neuroendocrinol.* 2023;35(12):e13343. doi:10.1111/jne.13343
  25. Lamarca A, Bartsch DK, Caplin M, et al. European neuroendocrine tumor society (ENETS) 2024 guidance paper for the management of well-differentiated small intestine neuroendocrine tumours. *J Neuroendocrinol.* 2024;36:e13423. doi:10.1111/jne.13423
  26. Pusceddu S, Prinzi N, Tafuto S, et al. Association of upfront peptide receptor radionuclide therapy with progression-free survival among patients with enteropancreatic neuroendocrine tumors. *JAMA Netw Open.* 2022;5(2):e220290. doi:10.1001/jamanetworkopen.2022.0290
  27. Singh S, Halperin D, Myrehaug S, et al. [177Lu]Lu-DOTA-TATE plus long-acting octreotide versus high-dose long-acting octreotide for the treatment of newly diagnosed, advanced grade 2-3, well-differentiated, gastroenteropancreatic neuroendocrine tumours (NETTER-2): an open-label, randomised, phase 3 study. *Lancet.* 2024;403(10446):2807-2817. doi:10.1016/s0140-6736(24)00701-3
  28. Panzuto F, Pusceddu S, Faggiano A, et al. Prognostic impact of tumour burden in stage IV neuroendocrine neoplasia: a comparison between pancreatic and gastrointestinal localizations. *Pancreatol.* 2019;19(8):1067-1073. doi:10.1016/j.pan.2019.09.015
  29. Caruso D, Zeranian M, Pucciarelli F, et al. Influence of adaptive statistical iterative reconstructions on CT radiomic features in oncologic patients. *Diagnostics.* 2021;11(6):1000. doi:10.3390/diagnostics11061000

**How to cite this article:** Polici M, Caruso D, Masci B, et al. Radiomics in advanced gastroenteropancreatic neuroendocrine neoplasms: Identifying responders to somatostatin analogs. *J Neuroendocrinol.* 2024;e13472. doi:10.1111/jne.13472